Nat. Hazards Earth Syst. Sci. Discuss., 3, 7379–7409, 2015
www.nat-hazards-earth-syst-sci-discuss.net/3/7379/2015/
doi:10.5194/nhessd-3-7379-2015
© Author(s) 2015. CC Attribution 3.0 License.

Natural Hazards and Earth System Sciences
Open Access
Discussions

This discussion paper is/has been under review for the journal Natural Hazards and Earth System Sciences (NHESS). Please refer to the corresponding final paper in NHESS if available.

Magnitude and frequency of heat and cold waves in recent decades: the case of South America

G. Ceccherini[1], S. Russo[1], I. Ameztoy[1], C. P. Romero[2], and C. Carmona-Moreno[1]

[1]DG Joint Research Centre, European Commission, Ispra 21027, Italy
[2]Facultad de Ingeniería Ambiental, Universidad Santo Tomás, Bogota 5878797, Colombia

Received: 12 November 2015 – Accepted: 23 November 2015 – Published: 10 December 2015

Correspondence to: G. Ceccherini (guido.ceccherini@ext.jrc.ec.europa.eu)

Published by Copernicus Publications on behalf of the European Geosciences Union.

Abstract

In recent decades there has been an increase in magnitude and occurrence of heat waves and a decrease of cold waves which are possibly related to the anthropogenic influence (Solomon et al., 2007). This study describes the extreme temperature regime of heat waves and cold waves across South America over recent years (1980–2014). Temperature records come from the Global Surface Summary of the Day (GSOD), a climatological dataset produced by the National Climatic Data Center that provides records of daily maximum and minimum temperatures acquired worldwide. The magnitude of heat waves and cold waves for each GSOD station are quantified on annual basis by means of the Heat Wave Magnitude Index (Russo et al., 2014) and the Cold Wave Magnitude Index (CWMI, Forzieri et al., 2015). Results indicate an increase in intensity and in frequency of heat waves, with up to 75 % more events occurring only in the last 10 years. Conversely, no significant changes are detected for cold waves. In addition, the trend of the annual temperature range (i.e., yearly mean of Tmax – yearly mean of Tmin) is positive – up to 1 °C decade^{-1} – over the extra-tropics and negative – up to 0.5 °C decade^{-1} – over the tropic. This dichotomous behaviour indicates that the annual mean of Tmax is generally increasing more than the annual mean of Tmin in the extra-tropics and viceversa in the tropics.

1 Introduction

In the coming decades, climate change will expose hundreds of millions of people to its impacts (Pachauri et al., 2014; Solomon et al., 2007; WHO, 2015). Many areas will have to deal with increases in temperature and changes in extreme weather conditions such as heat waves, altering the probability of experiencing major heat waves in the very near future (Field et al., 2012). This, in turn, may lead to serious implications, mainly health- and health-service-related (Barnett et al., 2012; Conti et al., 2005; Ostro et al.,

NHESSD
3, 7379–7409, 2015

CC BY

2009). The 2003 European heat wave (Beniston, 2004) illustrated how infrastructures, even in highly developed countries, can fail to deal with such environmental challenges.

Under this perspective, variability and changes in extreme temperature regimes present a considerable challenge for South America (Magrin et al., 2014). Different aspects of the occurrence of temperature extremes – both spatially and temporally – are still lacking for the continent (Rusticucci, 2012). A complete picture, along with a robust assessment, of temperature extreme regimes might provide essential information on the climate-related risks that society now faces, and how these risks are changing.

Amongst the areas of South America most vulnerable to heat and cold waves are the so-called "mega-cities", i.e. metropolitan areas with total population in excess of ten million people such as Bogota, Sao Paulo, Rio de Janeiro and Buenos Aires. Climate change issues are thus coupled with anthropic pressure issues.

In order to study extreme temperature regimes, daily records are needed. This requirement is particularly hard to meet in South America, which has a sparse gauge network. To overcome this problem, the Global Surface Summary of the Day (GSOD) meteorological dataset has been employed. GSOD is a compilation of daily meteorological data produced by the National Climatic Data Center, available from 1929 to present, which displays a reasonably dense coverage across South America. GSOD has been recently employed to show an increases in the number of heat waves in urban areas at the global scale (Mishra et al., 2015).

The aim of this paper is twofold. Firstly, to calculate annual magnitudes of heat waves and cold waves during 1980–2014 using maximum and minimum daily temperature from GSOD meteorological records. Secondly, to estimate trends of maximum, minimum temperature, and their relative range across South America. These analyses put in evidence different aspects of temperature extremes, still largely unknown across South America.

The analysis presented below follows a three step procedure that is divided as follows: (1) selection of temperature records with at least 30 years of data (see Sect. 2.2.1), (2) calculation of the Heat Wave Magnitude Index (HWMI) and Cold Wave

CC BY

Magnitude Index (CWMI) for the period 1980–2014, (3) estimation of the trend for annual mean of daily maximum temperature, annual mean of daily minimum temperature, and the Mean Temperature Range (i.e., MTR = annual mean of daily maximum – annual mean of daily minimum temperature, see Sect. 2.2 for further details).

2 Materials and methods

2.1 Materials: GSOD

Global Surface Summary of the Day (GSOD) is a product produced by the National Climatic Data Center (NCDC), derived from synoptic/hourly observations. GSOD records are mainly collected at international airports. GSOD records include mean, max, and min values of temperature, dew point, sea level and station atmospheric pressures, visibility, and wind speed including maximum sustained wind speed and/or wind gusts, precipitation amounts, snow depth, and indicators for occurrences of various weather elements such as fog, rain, snow, hail, thunder, and tornado. Historical data are generally available from 1929, with data from 1973 onwards being the most complete. The total number of GSOD stations available across South America is equal to 851. However, not all of them satisfy the condition of having at least a 30-year timespan, as needed to calculate heat and cold wave magnitude indices, as described in Sect. 2.2.1.

2.2 Methods

GSOD data are quality controlled through automated quality checks. Most random errors are removed and further corrections are applied, e.g. changes in instrumentation, station displacement to new locations. However, temperature acquisitions from GSOD are affected by missing data, therefore preventing the computation of the HWMI and CWMI which need a daily time series of at least 30 years. For this reason the stations with less than 30 years records and with more than 30 % of gaps have not been consid-

CC BY

ered in our data record. Figure 1 shows the spatial distribution of the 705 temperature stations that satisfy these conditions.

Table 1 details the distribution of the GSOD station and the ratio between available and used stations for each country, with the highest number of station in Brazil, and the lowest in French Guyana. The average of the ratio between used and available station is about 77 %, thus indicating a good coverage across the continent.

2.2.1 The heat and cold wave magnitude indices

Before the introduction of the Heat Wave Magnitude Index (HWMI, Russo et al., 2014), there was no consensus among researchers on the definition of heat waves (Perkins and Alexander, 2012). In fact, most of them take into account only partial aspects of the heat wave event such as maximum temperature, duration, or frequency, without considering the broader picture.

Recently, Russo et al. (2014), have introduced the HWMI able to overcome the limitation above by merging a few climate measures, as duration and temperature anomaly, into a single numerical index (Hoag, 2014). Basically, the magnitude index sums the probability scores associated to consecutive daily temperatures above the threshold. The HWMI computations requires a 30-year long time series of daily temperature records. The latter normally refers to the 1981–2010 timespan taken as reference period. In this work this index and the corresponding Cold Wave Magnitude Index (CWMI), defined below, are used to detect South American heat and cold waves in the present climate.

Following the definition of the HWMI in Russo et al. (2014), the CWMI (Forzieri et al., 2015) has been defined for each GSOD station by the following steps:

1. Daily threshold. For each day of the year, we define the daily threshold as the 10th percentile of the daily temperatures, centered on a 31 day window for the 30-year reference period 1981–2010.

CC BY

2. Cold wave selection. For each year, we select all the cold waves with at least three consecutive days below the daily thresholds.

3. Cold wave to subcold waves. We decompose each cold wave into x subcold waves, where a subcold wave is a three-day cold wave.

4. Subcold wave unscaled magnitude. For each subcold wave, we define the unscaled magnitude as the sum of the (three) daily temperatures.

5. Subcold wave scaled magnitude. For each subcold wave, we convert the unscaled magnitude to a probability ranging from 0 to 1, i.e. the scaled magnitude.

6. Cold wave magnitude. We define the magnitude of each cold wave as the sum of the scaled magnitudes of the x subcold waves.

7. Cold Wave Magnitude Index (CWMI). We define the CWMI for each year as the minimum of all cold wave magnitudes.

Both heat and cold waves are computed using: (1) maximum (hereafter $HWMI_{tx}$ and $CWMI_{tx}$), and (2) minimum (hereafter $HWMI_{tn}$ $CWMI_{tn}$) daily temperature, giving thus complementary information respectively on warm and cold day and night conditions. Heat and Cold Wave Magnitude Indices have been computed on annual basis for each GSOD station across South America for the period 1980–2014.

Since across South America heat waves generally occur between December and January, the calendar year used for HWMI starts in July and ends in June. In such manner we avoid splitting in two heat waves that happen at the end of December and the beginning of January. Therefore, the HWMI computation starts on 1 July 1980 and ends on 30 June 2015.

Similarly, since cold wave events are more likely to happen in the Southern Hemisphere between June and August, the calendar year used for CWMI computation starts on 1 January 1980 and ends on 31 December 2014.

CC BY

Heat wave and cold wave scale categories are defined with the classes set out in Table 2, following the scheme proposed by Russo et al. (2014) for heat waves. Note that the classification scheme for cold waves traces the one for heat waves, with negative values instead.

2.2.2 Trend of mean temperature range

Trend analysis has been carried out for each GSOD station applying the Mann–Kendall test to the time series of annual mean of daily maximum (Tx), daily minimum (Tn), and Mean Temperature Range (MTR). MTR is the difference between the annual mean of the daily maximum temperature and the annual mean of the daily minimum temperature. The intermittent nature of heat and cold waves prevents from carrying out trend analysis for HWMI and CWMI, even with such long time records.

MTR spans the high-temperature events of the summer season and the low-temperature events of the winter season. If the minimum temperature increases faster (slower) than the maximum, the temperature distribution becomes narrower (wider). Thus changes in MTR are mainly related to changes in the width of the average temperature distribution.

The Mann–Kendall trend test (Mann, 1945) allows us to detect significant trends in time series of temperature without assuming any particular distribution. Mann–Kendall test statistically assesses whether there is a positive or negative trend over time. As the test is non-parametric, it is less conditioned by outliers.

3 Results

3.1 Heat Wave

Figure 2 shows the maximum value in 5-year periods of the $HWMI_{tx}$ from 1980 to 2014. Histograms in the bottom-right corners show the distribution of the magnitude index for each 5-year period. Considering that maximum and minimum temperature are highly

NHESSD
3, 7379–7409, 2015

CC BY

correlated, results with $HWMI_{tn}$ do not differ significantly from those detected with the $HWMI_{tx}$ (see Supplement).

There is evidence that an increase of heat wave intensity is ongoing. Specifically, from 1995 onwards it is possible to observe heat wave spread across South America, with the maximum presence during 2010–2014. Between 1980 and 1984 there have been heat waves with magnitude equal to sixteen across the central part of the continent, mainly corresponding to Peru, whereas other regions do not show such great heat waves. In particular, in the austral summer of 1982–1983, during one of the strongest El Niño event (Cane, 1983) of the 20th century, the highest HWMI values in Peru were comparable with the HWMI peak of the 2003 European heat wave killing more than 70 000 people (Robine et al., 2008; Russo et al., 2014).

The central part of the continent also displays severe heat waves during 1995–1999 in correspondence with 1997–98 El Niño event (McPhaden, 1999), whereas the rest of the region does not presents patterns related to El Niño. Generally, HWMI's frequency is low until 1994, and then increases rapidly. This is noticeable from the analysis of the histograms, where the maximum value of the y axis (i.e., the occurrence of heat waves) rises from 20 to 150 heat wave events per 5-year period. Our results show that 35 % of the meteorological stations present intense heat waves with HWMI ≥ 2.

Histograms in Fig. 3 show the temporal distribution of heat wave for each class of magnitude. The five year time window allows us to better visualize the evolution of heat waves and to filter out the influence of El Niño on the occurrence of extreme events. Results confirm previous findings of Fig. 2.

The occurrence of heat waves generally increased in the last ten years. This is particularly true for the last 5 years period, when Tx, and Tn rise dramatically. Maximum temperature shows the highest number of heat waves (note that plots' scale of the y axis is logarithmic), while minimum temperature the lowest one. For maximum temperature, the increase in heat wave events occurred for all the magnitude classes. For minimum temperature it is possible to observe the upwards trend only for heat waves with magnitude greater than two, whereas the other classes are relatively stationary.

NHESSD
3, 7379–7409, 2015

CC BY

Between 2005 and 2014, the number of GSOD stations affected by moderate to extreme heat waves (i.e., HWMI ≥ 2) is equal to 360, ~ 75 % greater than in the previous period (1980–2004), when the total number of heat wave records was equal to 205.

Maximum temperature has the highest number of heat wave, with 1805 occurrences, minimum temperature the lowest one with 1025 occurrences. Note that this tally includes heat waves with HWMI greater than one (i.e., "normal" heat waves) that are not shown in both Figs. 2 and 3.

Figure 4 shows the $HWMI_{tx}$ for 2013 when Argentina, Uruguay, and Brazil experienced intense heat waves. Specifically, Argentina and Uruguay experienced extremely warm temperatures at the end of 2013 (Blunden and Arndt, 2014), whereas the cities of Sao Paulo and Rio de Janeiro (southeastern Brazil) experienced their warmest January and February at the beginning of 2014 (Blunden and Arndt, 2015). Note that 2013 refers to the period July 2013–June 2014, as explained in the method section. GSOD-derived observations are able to capture and quantify extreme weather events that occurred between 2013 and 2014. Annual maps of $HWMI_{tx}$ are provided in the Supplement.

3.2 Cold wave

As for heat waves, Fig. 5 shows the $CWMI_{tn}$ for 5-year periods from 1980 to 2014 (5-year maps for $CWMI_{tx}$ are shown in the Supplement). By means of the CWMI we were able to detect the strongest Cold Waves occurred in Latin America since 1980. It is possible to see that the vast majority of cold wave has a moderate magnitude with CWMI not below −3. Histograms in the bottom-right corners generally present an exponential decay of cold wave magnitude. Contrary to HWMI, it is not possible to distinguish an increase of cold wave intensity in the last decade.

Very extreme Cold waves (i.e., CWMI ≤ −8) are detected in correspondence to 1980–1984 and 1995–1999 periods across Ecuador and Venezuela. However, there is no temporal coherence with El Niño events (i.e., 1982–83 and 1997–98), since the

CC BY

major cold wave events took place during 1980 and 1996, respectively (Annual maps of $CWMI_{tn}$ are shown in the Supplement).

Just as for heat waves, histograms in Fig. 6 show the temporal distribution of cold waves for each class of magnitude. The occurrence of cold wave is essentially stationary across the weather stations. Only $CWMI_{tn}$ exhibits a positive trend in the 1980–1999 period, with a peak during 1995–1999, and a negative trend afterwards. Specifically, GSOD stations with $CWMI_{tn} \leq -2$ are nearly double the number for the other periods.

Differently from what found for heat waves, the CWMI applied to minimum and maximum temperatures have the same order of occurrence, with 1150 and 1187 events, respectively. Cold waves are observed for 35 % of the GSOD stations (i.e., about 250 stations).

3.3 Trend analysis

Figure 7 shows the slope of statistically significant trends, if any, of: (1) annual mean of daily maximum temperature, (2) annual mean of daily minimum temperature, and (3) Mean Temperature Range (MTR). Units are expressed as Celsius degrees per decade. Note that only stations with a statistically significant trend (i.e., p value smaller than 0.05, or 5 %) are shown, and the number of points changes accordingly. Interestingly, MRT displays trends in stations where there are no trends for both minimum and maximum temperature.

Annual mean of daily maximum temperature is generally increasing – up to $1\,^{\circ}\mathrm{C\,decade}^{-1}$ – across the continent: only few stations displays a negative trend. Annual mean of daily minimum temperature is increasing (up to $1\,^{\circ}\mathrm{C\,decade}^{-1}$) in the tropics (i.e., above -23° N), and decreasing (up to $0.5\,^{\circ}\mathrm{C\,decade}^{-1}$) in the extratropics. MTR displays a widening behavior in the extratropics, where the temperature range displays a broadening trend of up to $1\,^{\circ}\mathrm{C\,decade}^{-1}$. Conversely, spatial patterns of MTR's trends in the tropics indicate that negative trends generally prevail, with a few stations erratically showing positive trends. However, both spatial density and magni-

NHESSD
3, 7379–7409, 2015

CC BY

tude of negative trend across the tropics are less prominent than the positive ones in the South. The maximum reduction found in MTR is equal to 0.5 °C decade^{-1}.

The number of GSOD stations that display statistical significant trends for maximum temperature, minimum temperature, and MTR is about 15 % of the available stations.

3.4 Extreme temperatures over a mega-city: Bogota

In order to confirm our previous findings, the daily meteorological data pertaining to the Bogota have been analysed. Located in the tropics, Bogota and its metropolitan area is one of the four mega-cities of South America and represents one of the areas more at risk for extreme events (Instituto de Hidrología, Meteorología y Estudios Ambientales et al., 2014). The meteorological station is located in the El Dorado International Airport, 15 km north west of central Bogota.

Figures 8 and 9 show daily maximum and minimum temperatures, respectively. The average values (i.e., mean ±2 standard deviation) of the 1980–2014 time series are in black, the highest and lowest values in orange. Hence, for a given day d, the highest and the lowest values are defined by Eqs. (1) and (2):

$$T\_\text{highest}_d = \max \bigcup_{y=1980}^{2014} T_{y,d} \tag{1}$$

$$T\_\text{lowest}_d = \min \bigcup_{y=1980}^{2014} T_{y,d} \tag{2}$$

$\bigcup$ stands for the union of sets. $T_{y,d}$ is the daily maximum (minimum) temperature in the year y of the day d in Fig. 8 (Fig. 9).

NHESSD

3, 7379–7409, 2015

Magnitude and frequency of heat and cold waves in recent decades: the case of South America

G. Ceccherini et al.

The black lines in Figs. 8 and 9 represent the daily average for 1980–2014 of maximum and minimum temperature, respectively:

$$T\_mean\_longterm_d = \text{mean} \bigcup_{y=1980}^{2014} T_{y,d} \tag{3}$$

Similarly, the red lines represent the daily average in the most recent 5-year period (i.e., 2010–2014):

$$T\_mean\_last5_d = \text{mean} \bigcup_{y=2010}^{2014} T_{y,d} \tag{4}$$

In the last 5 years our data show a shift towards warmer temperatures: in 2010–2014 daily temperature values are nearly always above the 1980–2014 average. This is particularly noticeable for minimum temperatures, upholding what we previously found across the tropics: Tn is increasing faster than Tx.

Two indicators are employed to evaluate the difference between the daily average in the most recent 5-year period and the daily average of the 1980–2014 period for maximum and minimum temperature: (1) the Root Mean Square Error (RMSE); and (2) the Absolute Error (Abs. Err).

$$\text{RMSE} = \sqrt{\frac{\sum_{i=1}^{d} (T\_mean\_last5_d - T\_mean\_longterm_d)^2}{d}} \tag{5}$$

$$\text{Abs. Err} = \frac{1}{d} \sum_{i=1}^{d} |T_{\text{mean}}\_last5_d - T\_mean\_longterm_d| \tag{6}$$

Where T_mean_last5$_d$ and T_mean_longterm$_d$ represent respectively daily average in the most recent 5-year period and daily average in the 1980–2014 period, while d is the calendar day ranging from 1 to 365.

NHESSD
3, 7379–7409, 2015

CC BY

The RMSE ranges from 0.79 °C (Tx) to 1.11 °C (Tn), whereas the Abs. Err varies from 0.63 °C (Tx) to 1.30 °C (Tn).

4 Discussion

Our work is as an attempt towards temperature regime characterization for South America, and presents a number of caveats thereof.

Firstly, the spatial distribution of GSOD station is a critical aspect. GSOD stations are unevenly distributed across the region. However, spatial distribution of temperature, especially at daily level, is a major issue for this region with such a sparse network. Definitively, GSOD dataset represents the state of the art of daily temperature records across South America where large gaps exist (e.g., records were interrupted, or stations were removed). This is of course an issue that cannot be rectified, and only reanalysis products might help in producing consistent pictures of the region.

Secondly, it is likely that land use changes such as urbanization or large agricultural expansion induce abrupt changes or jumps in the time series of temperature (Zhou et al., 2014), and these aspects has not been taken into account in our study. However, trends and abrupt changes cannot be easily distinguished in statistical tests (Yevjevich, 1987) since they are very closely intertwined.

Thirdly, trend analysis presented in this study, cannot predict future climate patterns completely accurately. Caution should be exercised: evidence from longer records, instrumental or proxy, suggest that local trends are omnipresent but not monotonic; rather that at some time upward trends turn to downward ones and vice versa (Montanari and Koutsoyiannis, 2014).

Fourthly, the location of the meteorological stations can certainly affect the temperatures recorded. GSOD records, which often pertain to urban areas, are subject to the urban island effect that influences the recorded surface air temperatures, as shown across the US by Fall et al. (2011) and at global scale by Kalnay and Cai (2003).

CC BY

That being said, our analysis provides a unique research opportunity to explore observed extreme temperature regimes across South America, reducing spatial and temporal gaps on heat and cold waves and their trends (Perkins, 2015). This analysis takes advantage of the state-of-the-art technique developed in heat wave (Hoag, 2014) and cold wave (Forzieri et al., 2015) assessment. This analysis gives a perspective on cold waves, which has been rarely studied.

There is evidence of an ongoing increase in intensity and frequency of heat wave events. Specifically, from 1995 onwards it is possible to observe heat wave spread with the maximum presence during 2010–2014. In the last ten years (i.e., 2005–2014), the number of GSOD stations experiencing heat waves is ~ 75 % greater than in the previous 25-year long period (i.e., 1980–2004). Interestingly, the spatial patterns of heat wave across Peru display a correspondence with El Niño events (Carmona-Moreno et al., 2005), whereas the rest of the continent does not show such great similarities.

Maximum temperature displays the highest number of heat waves, minimum temperature the lowest one. Interestingly, the HWMI applied to minimum temperature displays lower magnitude than the HWMI values calculated with daily maximum; and there are no evident trends in the temporal distribution of heat waves with magnitude index greater than three. This might be due to the rapid night-time cooling, especially along the ocean coastline.

The occurrence of cold wave is essentially stationary in the sense of both intensity and frequency, with the exception of minimum temperature. In this regard, it is possible to observe an upward trend, with the peak between 1995 and 1999, turning downwards afterwards. Specifically, the number of GSOD stations with CWMI less or equal to −2 during 1995–2000 is twice the number of events during the other periods. Cold waves do not display temporal coherence with El Niño events. Apparently, there are no similarities between La Niña events, volcanic eruptions, such as the Pinatubo eruption of 1991, and cold waves across South America.

Annual mean of daily maximum temperature is generally increasing, up to 1 °C decade^{-1}, whereas annual mean of daily minimum temperature is increasing (up to

CC BY

1 °C decade^{-1}) in the tropics, and decreasing (up to 0.5 °C decade^{-1}) in the extratropics. Also MTR displays an opposed latitude-dependent behaviour. MTR shows a broadening trend up to 1 °C decade^{-1} in the extratropics, while negative trends generally prevail in the tropics, with a reduction up to 0.5 °C decade^{-1}. Generally minimum temperature shows interannual variability higher than maximum temperature, as shown in Figs. 8 and 9. This effect might hinder the trend detection of minimum temperature, especially when the relative trend is included in the range of variability.

Results support the findings of Mishra et al. (2015): the number of heat waves has increased. The occurrence of heat waves with a magnitude index greater than two has been most prominent in the most recent period. Results also support what was reported in Kenyon and Hegerl (2008): temperature extremes are substantially affected by El Niño.

Generally, there is agreement with Rusticucci (2012) on the positive trends of warm night (i.e. heat waves of minimum temperature), even if the trend of heat waves related to maximum temperature is more pronounced.

Finally, coherence with IPCC 2007 findings (Solomon et al., 2007) has been examined. The IPCC theoretical prediction for increasing in maximum temperature are coherent with our results. Conversely, in our study the dramatic rise of daily minimum temperatures, projected to increase faster than daily maximum temperatures, has been found only over the tropics.

5 Conclusions

This study assesses the specific behavior of extreme temperature regimes from the Global Summary of Day (GSOD) database recorded across South America in the period 1980–2014. Analysis of the extreme values and trends of interannual ranges of temperatures are crucial since it gives insight into “outside-of-the-box” scenarios (Lagadec, 2004) which very few studies consider. Applications of these analyses are man-

NHESSD
3, 7379–7409, 2015

CC BY

ifold in essential sectors such as local health and social care system (Carmichael et al., 2012; Gupta and Gregg, 2012).

Heat and cold waves are calculated using the Heat Wave Magnitude Index (Russo et al., 2014) and the Cold Wave Magnitude Index (i.e., CWMI) obtained by adapting the HWMI as an equivalent indicator, for maximum and minimum daily temperatures. Finally, trend detection has been performed to assess the significance of temporal changes in the annual mean of daily maximum temperature, annual mean of daily minimum temperature, and the Mean Temperature Range (i.e., MTR).

Results from heat wave analysis indicates the presence of an increase in intensity and in frequency of extreme events, with up to 75 % more events occurring only in the last 10 years. Results from cold wave analysis show an erratic behavior and no conclusion can be drawn. Heat wave shows temporal coherence with El Niño events (i.e., 1982–1983 and 1997–1998), whereas no connection between cold waves and El Niño can be inferred from our analysis.

MTR‘s trends indicate that the maximum temperature is generally increasing faster than the minimum temperature over the extratropics. Across the tropics, the interannual ranges of mean temperature are generally narrowing, even if the corresponding spatial patterns are not outstandingly noticeable.

The outcomes described in this paper open the possibility to extend the presented scheme over very long periods worldwide. Further applications include the study of the impact of land use changes on heat waves and differential increases in temperature. Other applications of the paper includes the employment of GSOD records as an independent check that temperature reconstructions produced using reanalysis data such as ERA-INTERIM (Dee et al., 2011) are in-line with raw data from observational stations.

The Supplement related to this article is available online at doi:10.5194/nhessd-3-7379-2015-supplement.

CC BY

Acknowledgements. Authors would like to thank the valuable support from JRC. This work has received funding from European Commission EuropeAid Co-operation Office under grant agreements EUROCLIMA and RALCEA. The data used in this manuscript can be obtained from Global Summary of the Day (GSOD) version 8, National Climatic Data Center (ftp://ftp.ncdc.noaa.gov/pub/data/gsod/). The code used to produce Bogota's daily temperature graphic has been provided by http://rpubs.com/bradleyboehmke/weather_graphic. Heat and Cold Wave Magnitude Indices have been computed using the R library "extRemes" (Gilleland, 2015). Google data are registered trademarks of Google Inc., used with permission.

References

Barnett, A. G., Hajat, S., Gasparrini, A., and Rocklöv, J.: Cold and heat waves in the United States, Environ. Res., 112, 218–224, doi:10.1016/j.envres.2011.12.010, 2012.

Beniston, M.: The 2003 heat wave in Europe: a shape of things to come? An analysis based on Swiss climatological data and model simulations, Geophys. Res. Lett., 31, L02202, doi:10.1029/2003GL018857, 2004.

Blunden, J. and Arndt, D. S.: State of the climate in 2013, B. Am. Meteorol. Soc., 95, S1–S279, doi:10.1175/2014BAMSStateoftheClimate.1, 2014.

Blunden, J. and Arndt, D. S.: State of the climate in 2014, B. Am. Meteorol. Soc., 96, ES1–ES32, doi:10.1175/2015BAMSStateoftheClimate.1, 2015.

Cane, M. A.: Oceanographic events during El Niño, Science, 222, 1189–1195, 1983.

Carmichael, C., Bickler, G., Kovats, S., Pencheon, D., Murray, V., West, C., and Doyle, Y.: Overheating and hospitals – what do we know?, J. Hosp. Adm., 2, 1–7, doi:10.5430/jha.v2n1p1, 2012.

Carmona-Moreno, C., Belward, A., Malingreau, J.-P., Hartley, A., Garcia-Alegre, M., Antonovskiy, M., Buchshtaber, V., and Pivovarov, V.: Characterizing interannual variations in global fire calendar using data from Earth observing satellites, Glob. Change Biol., 11, 1537–1555, doi:10.1111/j.1365-2486.2005.01003.x, 2005.

Conti, S., Meli, P., Minelli, G., Solimini, R., Toccaceli, V., Vichi, M., Beltrano, C., and Perini, L.: Epidemiologic study of mortality during the summer 2003 heat wave in Italy, Environ. Res., 98, 390–399, doi:10.1016/j.envres.2004.10.009, 2005.

CC BY

Dee, D. P., Uppala, S. M., Simmons, A. J., Berrisford, P., Poli, P., Kobayashi, S., Andrae, U., Balmaseda, M. A., Balsamo, G., Bauer, P., Bechtold, P., Beljaars, A. C. M., van de Berg, L., Bidlot, J., Bormann, N., Delsol, C., Dragani, R., Fuentes, M., Geer, A. J., Haimberger, L., Healy, S. B., Hersbach, H., Hólm, E. V., Isaksen, L., Kållberg, P., Köhler, M., Matricardi, M., McNally, A. P., Monge-Sanz, B. M., Morcrette, J.-J., Park, B.-K., Peubey, C., de Rosnay, P., Tavolato, C., Thépaut, J.-N., and Vitart, F.: The ERA-Interim reanalysis: configuration and performance of the data assimilation system, Q. J. Roy. Meteor. Soc., 137, 553–597, doi:10.1002/qj.828, 2011.

Fall, S., Watts, A., Nielsen-Gammon, J., Jones, E., Niyogi, D., Christy, J. R., and Pielke, R. A.: Analysis of the impacts of station exposure on the U.S. Historical Climatology Network temperatures and temperature trends, J. Geophys. Res.-Atmos., 116, D14120, doi:10.1029/2010JD015146, 2011.

Field, C. B., Barros, V., Stocker, T. F., and Dahe, Q.: Managing the Risks of Extreme Events and Disasters to Advance Climate Change Adaptation: Special Report of the Intergovernmental Panel on Climate Change, Cambridge University Press, Cambridge, available at: https://books.google.it/books?id=BL6ouAAACAAJ (last access: 1 November 2015), 2012.

Forzieri, G., Feyen, L., Russo, S., Vousdoukas, M., Alfieri, L., Outten, S., Migliavacca, M., Bianchi, A., Rojas, R., and Cid, A.: Multi-hazard assessment in Europe under climate change, Clim. Change, submitted, 2015.

Gilleland, E.: extRemes: Extreme Value Analysis, available at: https://cran.r-project.org/web/packages/extRemes/index.html (last access: 9 September 2015), 2015.

Gupta, R. and Gregg, M.: Using UK climate change projections to adapt existing English homes for a warming climate, Build. Environ., 55, 20–42, doi:10.1016/j.buildenv.2012.01.014, 2012.

Hoag, H.: Russian summer tops "universal" heatwave index, Nature, doi:10.1038/nature.2014.16250, 2014.

Instituto de Hidrología, Meteorología y Estudios Ambientales, IDEAM, DNP, MADS, Parques Nacionales Naturales de Colombia, Instituto Humboldt, Corpoguavio, Gobernación de Cundinamarca, CAR, Alcaldí a de Bogotá and PNUD (Eds.): Bogota and Cundinamarca Face to Climate Change: Strategy Summary and Main Results of the Proces, PNUD, Bogotá, 2014.

Kalnay, E. and Cai, M.: Impact of urbanization and land-use change on climate, Nature, 423, 528–531, doi:10.1038/nature01675, 2003.

Kenyon, J. and Hegerl, G. C.: Influence of modes of climate variability on global temperature extremes, J. Climate, 21, 3872–3889, doi:10.1175/2008JCLI2125.1, 2008.

CC BY

Lagadec, P.: Understanding the French 2003 Heat Wave Experience: beyond the heat, a multi-layered challenge, J. Contingencies Crisis Manag., 12, 160–169, doi:10.1111/j.0966-0879.2004.00446.x, 2004.

Magrin, G. O., Marengo, J. A., Boulanger, J.-P., Buckeridge, M. S., Castellanos, E., Poveda, G., Scarano, F. R., and Vicuña, S.: Central and South America, in: Climate Change 2014: Impacts, Adaptation, and Vulnerability. Part B: Regional Aspects. Contribution of Working Group II to the Fifth Assessment Report of the Intergovernmental Panel of Climate Change, edited by: Barros, V. R., Field, C. B., Dokken, D. J., Mastrandrea, M. D., Mach, K. J., Bilir, T. E., Chatterjee, M., Ebi, K. L., Estrada, Y. O., Genova, R. C., Girma, B., Kissel, E. S., Levy, A. N., MacCracken, S., Mastrandrea, P. R., and White, L. L., Cambridge University Press, Cambridge, UK and New York, NY, USA, 1499–1566, 2014.

Mann, H. B.: Nonparametric tests against trend, Econometrica, 13, 245–259, 1945.

McPhaden, M. J.: El Niño: the child prodigy of 1997–98, Nature, 398, 559–562, doi:10.1038/19193, 1999.

Mishra, V., Ganguly, A. R., Nijssen, B., and Lettenmaier, D. P.: Changes in observed climate extremes in global urban areas, Environ. Res. Lett., 10, 024005, doi:10.1088/1748-9326/10/2/024005, 2015.

Montanari, A. and Koutsoyiannis, D.: Modeling and mitigating natural hazards: stationarity is immortal!, Water Resour. Res., 50, 9748–9756, doi:10.1002/2014WR016092, 2014.

Ostro, B. D., Roth, L. A., Green, R. S., and Basu, R.: Estimating the mortality effect of the July 2006 California heat wave, Environ. Res., 109, 614–619, doi:10.1016/j.envres.2009.03.010, 2009.

Pachauri, R. K., Allen, M. R., Barros, V. R., et al.: Climate Change 2014: Synthesis Report. Contribution of Working Groups I, II and III to the Fifth Assessment Report of the Intergovernmental Panel on Climate Change, available at: http://epic.awi.de/37530/ (last access: 17 March 2015), 2014.

Perkins, S. E.: A review on the scientific understanding of heatwaves – their measurement, driving mechanisms, and changes at the global scale, Atmos. Res., 164–165, 242–267, doi:10.1016/j.atmosres.2015.05.014, 2015.

Perkins, S. E. and Alexander, L. V.: On the measurement of heat waves, J. Climate, 26, 4500–4517, doi:10.1175/JCLI-D-12-00383.1, 2012.

NHESSD

3, 7379–7409, 2015

Magnitude and frequency of heat and cold waves in recent decades: the case of South America

G. Ceccherini et al.

CC BY

Robine, J.-M., Cheung, S. L. K., Le Roy, S., Van Oyen, H., Griffiths, C., Michel, J.-P., and Herrmann, F. R.: Death toll exceeded 70,000 in Europe during the summer of 2003, C. R. Biol., 331, 171–178, doi:10.1016/j.crvi.2007.12.001, 2008.

Russo, S., Dosio, A., Graversen, R. G., Sillmann, J., Carrao, H., Dunbar, M. B., Singleton, A., Montagna, P., Barbola, P., and Vogt, J. V.: Magnitude of extreme heat waves in present climate and their projection in a warming world, J. Geophys. Res.-Atmos., 119, 12500–12512, doi:10.1002/2014JD022098, 2014.

Rusticucci, M.: Observed and simulated variability of extreme temperature events over South America, Atmos. Res., 106, 1–17, doi:10.1016/j.atmosres.2011.11.001, 2012.

Solomon, S., Intergovernmental Panel on Climate Change, Intergovernmental Panel on Climate Change, and Working Group I: Climate Change 2007: The Physical Science Basis? Contribution Of Working Group I To The Fourth Assessment Report of the Intergovernmental Panel on Climate Change, Cambridge University Press, Cambridge, UK, 2007.

WHO: Climate Change and Health, WHO, available at: http://www.who.int/mediacentre/factsheets/fs266/en/ (last access: 20 October 2015), 2015.

Yevjevich, V.: Stochastic models in hydrology, Stoch. Hydrol. Hydraul., 1, 17–36, doi:10.1007/BF01543907, 1987.

Zhou, W., Ji, S., Chen, T.-H., Hou, Y., and Zhang, K.: The 2011 heat wave in Greater Houston: effects of land use on temperature, Environ. Res., 135, 81–87, doi:10.1016/j.envres.2014.08.025, 2014.

NHESSD

3, 7379–7409, 2015

Magnitude and frequency of heat and cold waves in recent decades: the case of South America

G. Ceccherini et al.

cc BY

Table 1. Spatial distribution of GSOD station across South American countries.

Country	Available	used	Ratio used/available
Argentina	136	123	0.90
Bolivia	38	33	0.87
Brazil	334	281	0.84
Chile	70	61	0.87
Colombia	57	39	0.68
Ecuador	50	44	0.88
French Guiana	3	3	1.00
Guyana	8	1	0.13
Peru	37	29	0.78
Paraguay	36	29	0.81
Suriname	12	9	0.75
Uruguay	22	17	0.77
Venezuela	48	36	0.75

NHESSD
3, 7379–7409, 2015

Table 2. Classification of heat and cold wave (i.e., HWMI and CWMI) scale categories.

Classification	Heat Wave Magnitude Index	Cold Wave Magnitude Index
Normal	$1 \leq \text{HWMI} < 2$	$-1 \geq \text{CWMI} > -2$
Moderate	$2 \leq \text{HWMI} < 3$	$-2 \geq \text{CWMI} > -3$
Severe	$3 \leq \text{HWMI} < 4$	$-3 \geq \text{CWMI} > -4$
Extreme	$4 \leq \text{HWMI} < 8$	$-4 \geq \text{CWMI} > -8$
Very Extreme	$8 \leq \text{HWMI} < 16$	$-8 \geq \text{CWMI} > -16$
Super Extreme	$16 \leq \text{HWMI} < 32$	$-16 \geq \text{CWMI} > -32$
Ultra Extreme	$\text{HWMI} \geq 32$	$\text{CWMI} \leq -32$

NHESSD
3, 7379–7409, 2015

CC BY

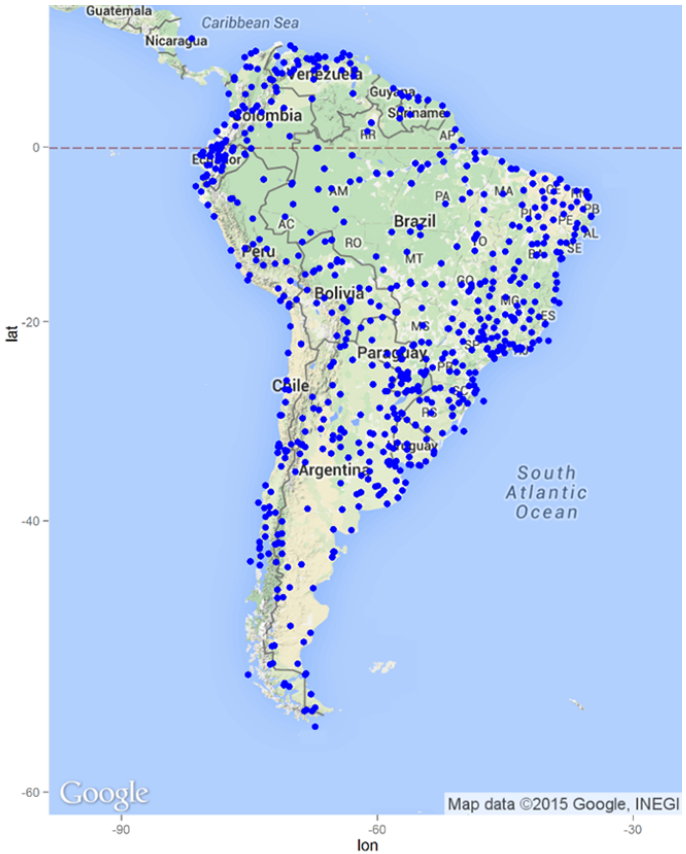

Figure 1. Spatial distribution of temperature gauges used in this study.

NHESSD

3, 7379–7409, 2015

CC BY

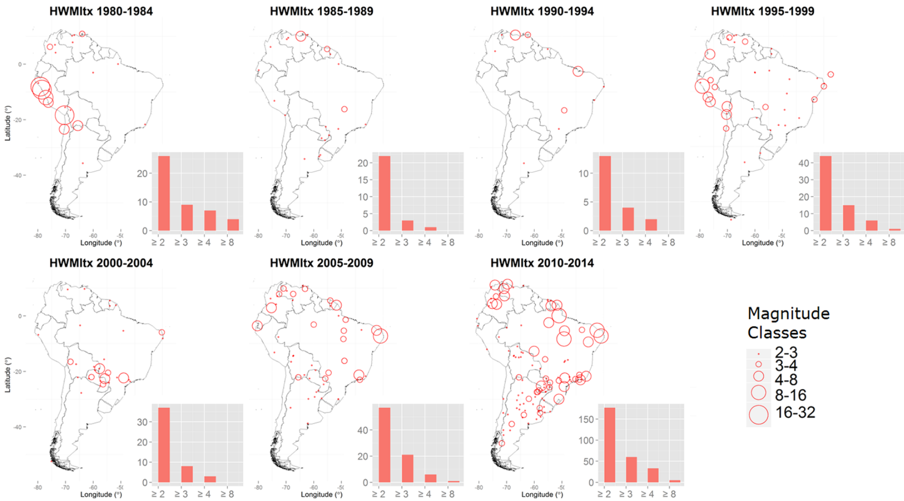

Figure 2. Magnitude of Heat Wave Index of maximum temperature ($HWMI_{tx}$) for 5-year periods from 1980 to 2014.

NHESSD
3, 7379–7409, 2015

Magnitude and frequency of heat and cold waves in recent decades: the case of South America

G. Ceccherini et al.

Title Page
Abstract | Introduction
Conclusions | References
Tables | Figures
◀| |▶
◀ ▶
Back | Close
Full Screen / Esc
Printer-friendly Version
Interactive Discussion

cc BY

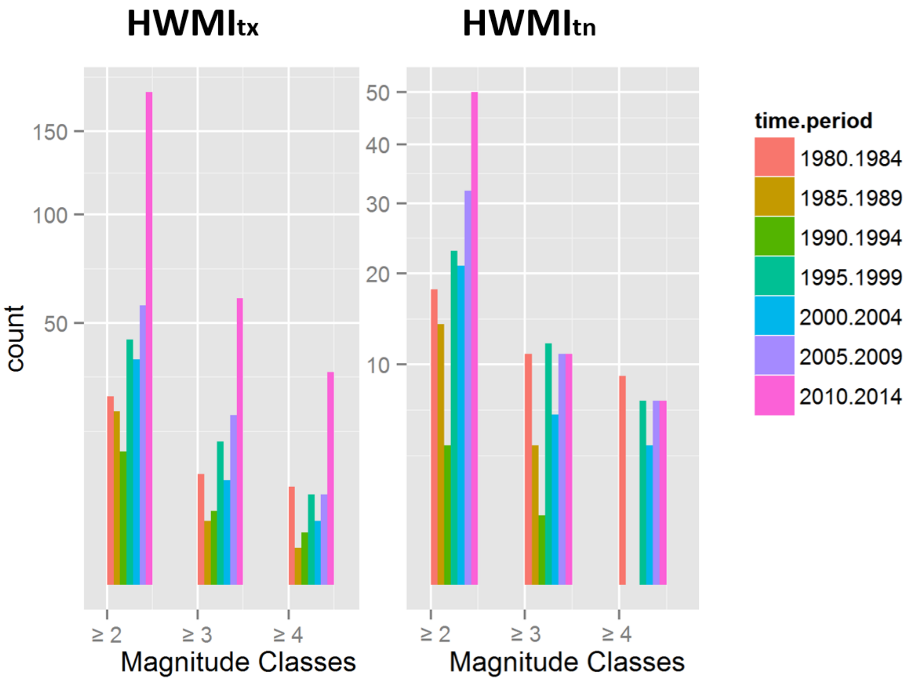

Figure 3. Histogram of heat wave for 5-year period during 1980–2014.

NHESSD
3, 7379–7409, 2015

Magnitude and frequency of heat and cold waves in recent decades: the case of South America

G. Ceccherini et al.

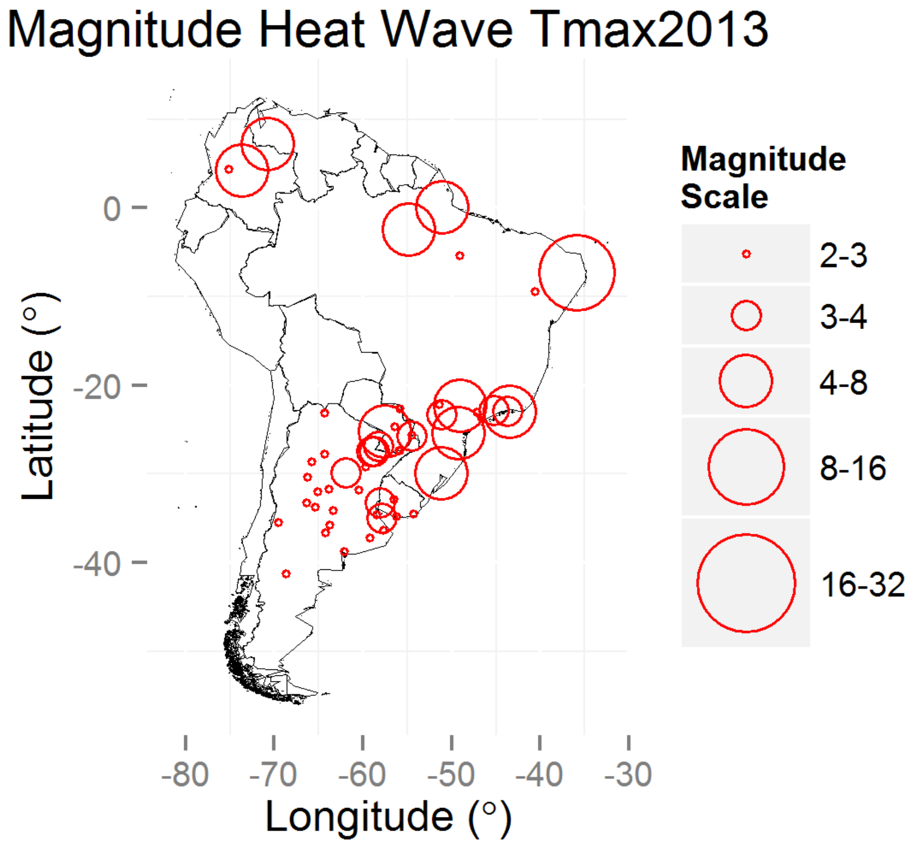

Figure 4. Magnitude of Heat Wave Index of maximum temperature ($HWMI_{tx}$) for 2013.

CC BY

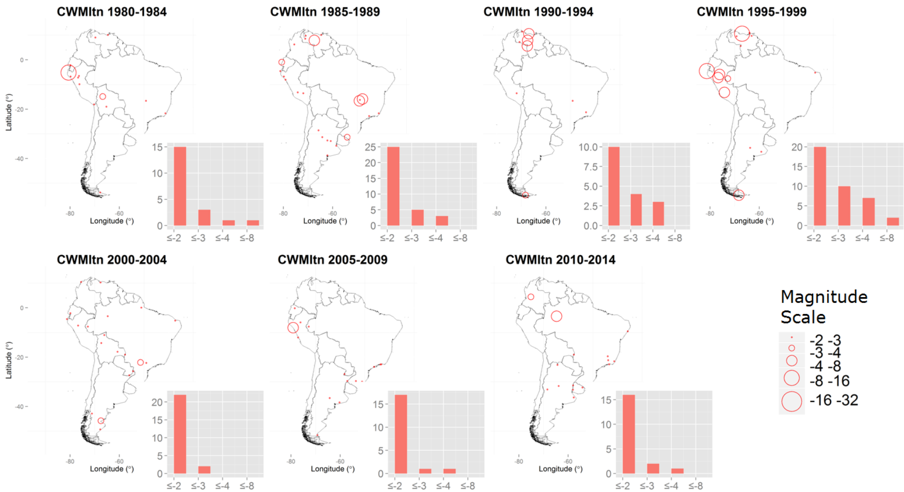

Figure 5. Magnitude of Cold Wave Index of minimum temperature ($CWMI_{tn}$) for 5-year periods from 1980 to 2014.

NHESSD
3, 7379–7409, 2015

Magnitude and frequency of heat and cold waves in recent decades: the case of South America

G. Ceccherini et al.

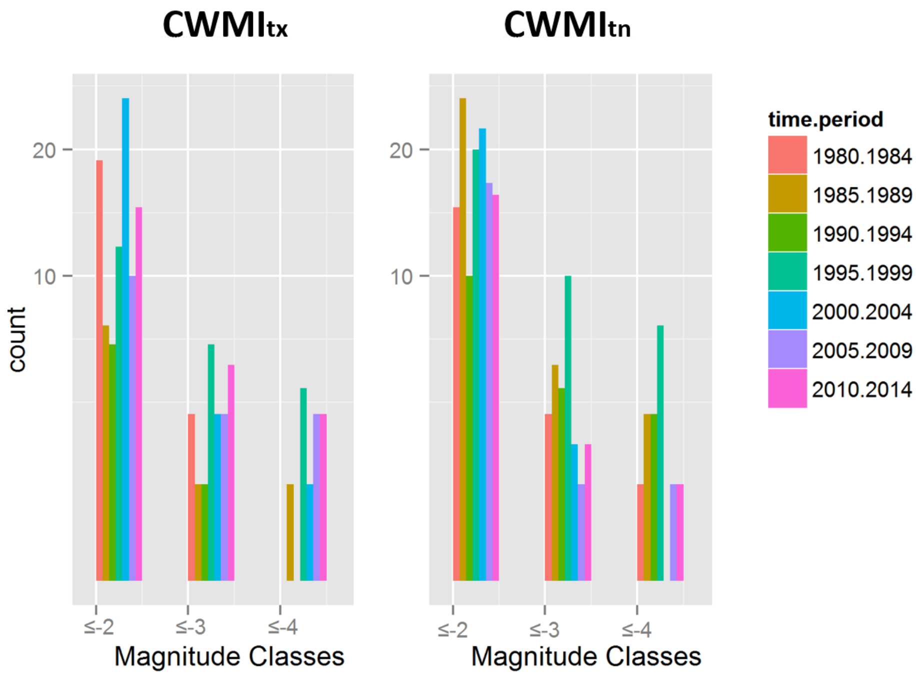

Figure 6. Histogram of cold wave for 5-year period during 1980–2014.

NHESSD
3, 7379–7409, 2015

CC BY

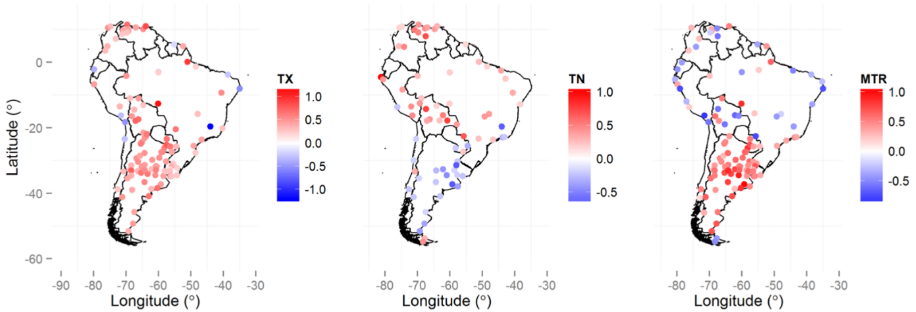

Figure 7. Trend in the mean annual maximum temperature (left panel), mean annual minimum temperature (central panel), and Mean Temperature Range (MTR, right panel). Units are expressed as Celsius degrees per decade.

NHESSD
3, 7379–7409, 2015

CC BY

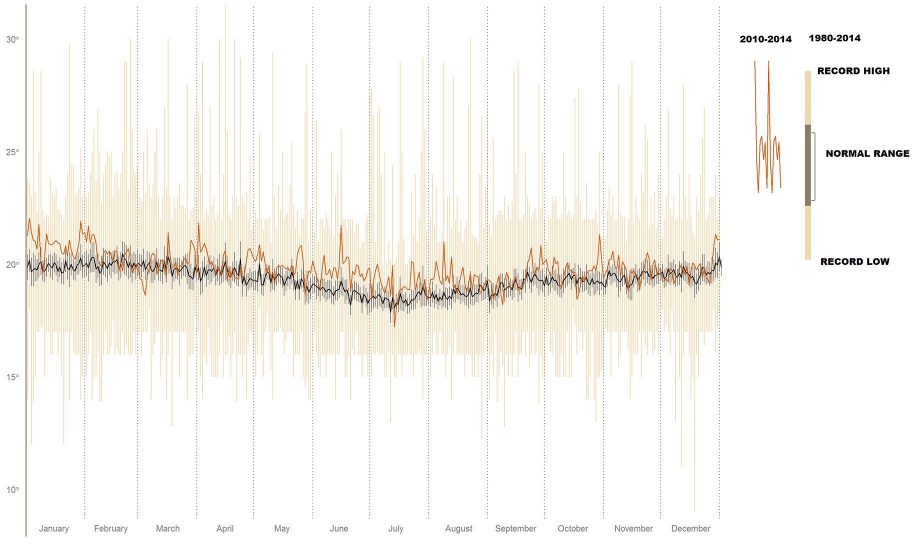

Figure 8. Bogota average of maximum daily temperature (2010–2014 vs. 1980–2014 values).

NHESSD
3, 7379–7409, 2015

Magnitude and frequency of heat and cold waves in recent decades: the case of South America

G. Ceccherini et al.

Title Page
Abstract | Introduction
Conclusions | References
Tables | Figures
◀| |▶
◀ ▶
Back | Close
Full Screen / Esc
Printer-friendly Version
Interactive Discussion

cc BY

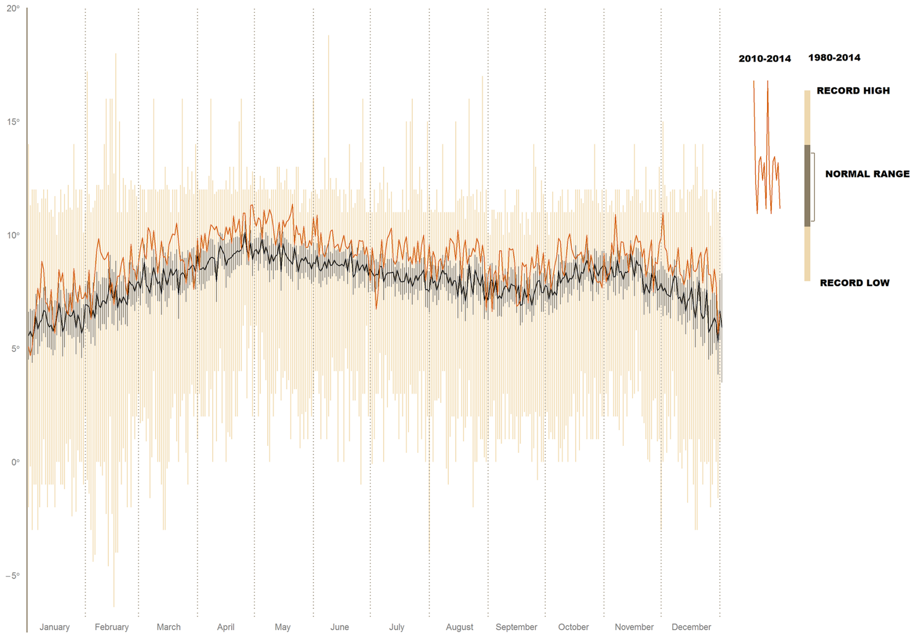

Figure 9. Bogota average of minimum daily temperature (2010–2014 vs. 1980–2014 values).

NHESSD
3, 7379–7409, 2015

Magnitude and frequency of heat and cold waves in recent decades: the case of South America

G. Ceccherini et al.

CC BY